# Voltage control of switched reluctance machines for Hybrid Electric Vehicles

B.A. Kalan, H.C. Lovatt and G. Prout

CSIRO Telecommunications & Industrial Physics
Bradfield road,
Lindfield NSW, Australia 2070

***Abstract*- The rugged low-cost construction and constant power profile of a switched reluctance motor (SRM) make it suitable for hybrid electric vehicles (HEVs). This paper describes the development of a voltage-based control strategy for a SRM. The controller design is influenced by project constraints and goals as well as the use of a new power topology. A prototype SRM and controller were built and fully tested to validate the SRM design and to develop a set of rules and equations for controlling the motor. Particular emphasis was given to developing a simple practical control strategy that was suitable for an HEV application and not trying to develop a more sophisticated strategy that could not be justified in terms of increased development time and implementation cost.**

## INTRODUCTION

Hybrid electric vehicles (HEVs) are attracting considerable interest, as they are a promising compromise solution to fill the gap between the conventional internal combustion engine (ICE) vehicle and the future purely electric vehicle, possibly powered by fuel cells. HEVs generally have an ICE, an electric machine and an electrical energy storage system. Compared to a conventional car, a HEV has reduced fuel consumption and lower emissions. This is primarily due to:

- a smaller more efficient ICE
- recovered energy from regenerative braking
- turning the ICE off at low load

The Commonwealth Scientific and Industrial Research Organisation (CSIRO) worked with the Australian automotive industry to develop two vehicles, the parallel hybrid *ECOmmodore* [1] (see Fig. 1) and series hybrid aXcessaustralia LEV [2]. These vehicles utilised a number of key CSIRO technologies that include light-metal casting, modelling of energy usage and pollution, an electrical storage system comprising of advanced lead-acid batteries and super-capacitors, and a novel power topology using switched reluctance motors (SRMs). The ECOmmodore has two motors and the aXcessaustralia LEV has three (all five motors used the same lamination, but the length and number of turns were different). The rugged low-cost construction, relatively high torque to mass ratio, and constant power profile of a SRM make it a good choice for HEV applications [3].

This paper describes the selection and development of a voltage-based control strategy for implementing average torque control of a SRM. The requirements for the controller in an HEV application were carefully considered and a series of experimental measurements were performed on a prototype SRM to formulate a control strategy and structure. Finally, each controller was customised to its own SRM.

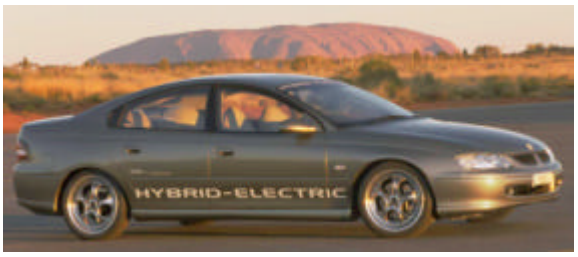


Fig. 1. Holden ECOmmodore

## POWER TOPOLOGY (ECOMMODORE CAR)

A new power topology [4] was conceived for the vehicles (see Fig. 2). This topology is believed to be a cost-effective way of implementing a system with multiple electrical energy storage units. It features two separate electric motors mounted on a common shaft, each motor is associated with a different electrical energy storage unit (namely batteries and super-capacitors).

Both the battery and super-capacitor units can motor or dynamically brake. Therefore it is possible to transfer power bi-directionally between the wheels, batteries, or super-capacitors. The ICE transfers power uni-directionally, only delivering power to the wheels, batteries, or super-capacitors. The peak power rating of the capacitor drive unit (see Fig. 3) is 32 kW and its main function is to provide or accept short bursts of power for accelerating or decelerating. Whereas, the peak power rating of the battery drive unit is 10 kW and it provides a larger energy capacity at lower power levels. The energy management computer (EMC) communicates with all of the car systems to decide the torque required from the battery and capacitor drive units. Mathematical modelling was performed with various driving cycles to determine the optimum rating of each SRM (see Table I).

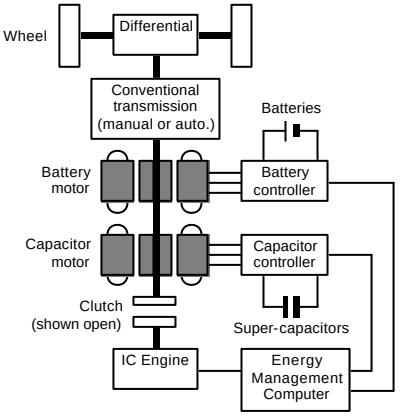


Fig. 2. Power topology for the ECOmmodore

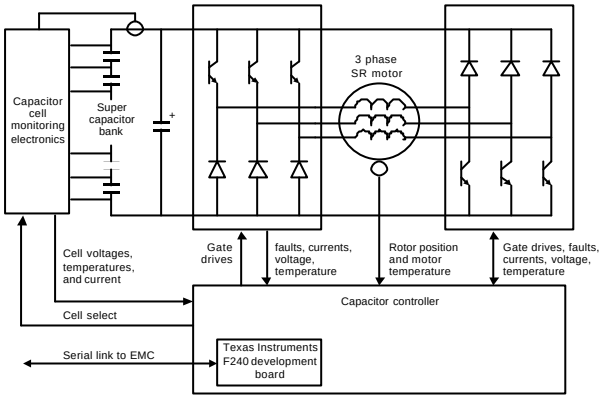


Fig. 3. Capacitor unit

TABLE I
SUMMARY OF SRM RATINGS

| HEV | ECOmmodore | | aXcessaustralia LEV | | |
|---|---|---|---|---|---|
| SRM | Capacitor Motor | Battery Motor | Main Motor | Capacitor Motor | Battery Motor |
| Peak Torque (Nm) | 80 | 25 | 140 | 90 | 30 |
| Peak power (kW) | 32 | 10 | 50 | 33 | 11 |
| Continuous power (kW) | 16 | 5 | 25 | 16.5 | 5.5 |
| Base speed (rpm) | 3820 | 3820 | 3440 | 3440 | 3440 |
| Maximum speed (rpm) | 5730 | 5730 | 7640 | 7640 | 7640 |

## MOTOR CONTROL CONSTRAINS AND REQUIREMENTS

The Texas instruments TMS320F240 digital signal processor (DSP) was selected early in the project due to its relatively fast instruction cycle time (50 ns) and its rich set of on-board peripherals specifically intended for motor control. It was also desirable to use one TMS320F240 DSP with its standard development board per unit (capacitor unit, battery unit, EMC). In addition to performing the motor control algorithm, the TMS320F240 DSP had to monitor and protect the battery or capacitor bank (104 cells in the capacitor bank), perform serial communications with the EMC, and protect the motor and power electronics. A simple motor control algorithm was desirable for many reasons, including: aggressive time schedules and fixed dates for promotional activities, all software to be written in 'C', limited processing time and memory availability, a reasonably high motor fundamental frequency of 800Hz, the total car system complexity, etc.

The mechanical arrangement of the two SRMs and the ICE on the same shaft favors the use of torque as the control variable. Therefore the EMC requests a torque and the motor controller must use a model or algorithm to try to deliver that torque. The required accuracy of average torque control is not very high. An error of 10% is acceptable, as the driver (performing the speed control) would not notice variations of this magnitude. Also, the dynamic response of the control loop can be quite slow (around 100 ms), due to the ratio of the car inertia to the torque output of the drive train. It was also believed that torque ripple reduction techniques, such as in [5] and [6], are not necessary in this application. These techniques typically control the current or flux waveforms applied to a phase and are computationally intensive and require more development effort. Constant torque is not required for control purposes, as the large inertia of the car effectively smoothes out the torque ripple of the SRM. Constant torque was not required for acoustic reasons either, as the ECOmmodore in electric mode was marginally too quiet for the safety of pedestrians accustomed to the sound of conventional cars.

After considering the points above it was decided to pursue the use of a voltage control structure. This provides the additional benefits of constant-frequency pulse width modulation (PWM), and enables the use of a low resolution rotor position sensing system utilising hall effect sensors intended for the automotive environment (many SRM controllers use high resolution optical encoders which were not desirable in this application for reliability, mechanical and cost reasons). If the SRM phase resistance is neglected, voltage control applies a ramping flux waveform to the phase, which can be a reasonable waveform for high motor efficiency. Also, at high power levels when the motor efficiency is most important, all typical control algorithms must saturate and essentially become voltage control, due to the limited dc link voltage.

## PROPOSED SRM CONTROLLER STRUCTURE

Fig. 4 shows the proposed control structure with an inner PWM and commutation control loop implemented with a Xilinx XC9572 programmable logic device and an outer torque controller implemented in the F240 DSP. The commutation technique turns a motor phase on at a rotor angle $\theta_{on}$ and then turns the phase off at a rotor angle $\theta_{off}$. If the dc link voltage and load conditions are constant, the PWM applied to the motor phase is constant while the phase is on. When the rotor passes $\theta_{off}$, the phase is turned off which applies the full negative dc link voltage to the motor phase until the phase current is reduced to zero. Generally, $\theta_{on}$ and $\theta_{off}$ are advanced with increasing speed and load torque. The digital position code ($\theta$) from the SRM gives the ability to set $\theta_{on}$ and $\theta_{off}$ in increments of 30°(electrical). This resolution was experimentally found to be a good trade-off between SRM performance and system complexity. The commutation control also implements a fast maximum current limit to protect the inverter and to limit the SRM torque and power.

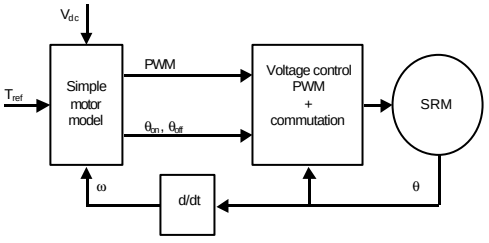


Fig. 4. Voltage controller

## LOADING RIG TESTS WITH THE PROTOTYPE SRM

Search techniques were used with finite element analysis (FEA) to design the three-phase SRMs [7] and loading rig tests were performed on a prototype SRM to confirm the machine design. The motor tests validated the design, and the measured torque, power and efficiency curves are shown in Fig. 5 and Fig. 6. The motor was not tested to its full power capability due to the limits of our loading rig. The inverter power loss was typically 3%. Five different commutation settings (C1, C2, C3, C4, C5) were required to cover the torque speed range and maintain motor efficiency. Commutation C1 turns the phase on when the rotor and stator teeth are unaligned ($\theta_{on}$ = 180°) and turns the phase off when the teeth are aligned ($\theta_{off}$ = 0°). Commutation C1 is always used when starting from rest. Commutation C2 is $\theta_{on}$ = 180° and $\theta_{off}$ = 30°, commutation C3 is $\theta_{on}$ = 210° and $\theta_{off}$ = 60°, and commutation C4 and C5 have progressively earlier turn on and off angles.

If magnetic non-linearity and mutual coupling are neglected, the torque from a single phase with current $i$, inductance $L$, and rotor angle $q$ is:

$$T = \frac{i^2}{2}\frac{\partial L}{\partial q} \qquad (1)$$

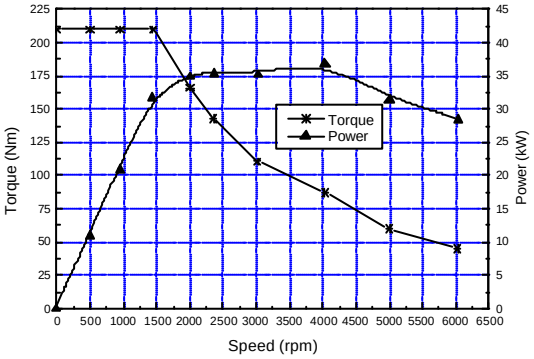


Fig. 5. Maximum torque and power for the prototype SRM

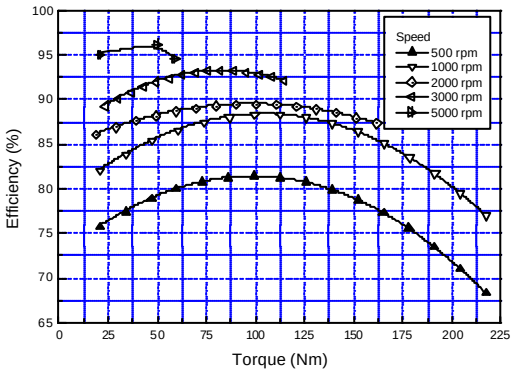


Fig. 6. Motor efficiency for the prototype SRM

This equation approximately agrees with the measured results. For example, the torque versus current relationship for commutation C2 and C3 at particular speeds are shown in Fig. 7 and Fig. 8, respectively. Below 50 Nm the curves follow a square law as indicated by (1) and above 50 Nm the magnetic circuit begins to experience local saturation resulting in a roughly linear relationship between torque and current. The departure from a straight line (in the region above 50 Nm) is more pronounced for commutation C2 (Fig. 7) than for C3 (Fig. 8). This characteristic of commutation C2 is due to bulk saturation of the machine at high torques (see the section of the current waveform marked with an arrow in Fig. 9) and due to pulses of negative torque at high powers (see the arrow in Fig. 10). As these effects become more dominant the motor efficiency for commutation C2 becomes lower than the motor efficiency for commutation C3, so at this point it is beneficial to change from commutation C2 to C3. The change in efficiency with operating conditions is relatively gradual, so there is some latitude in the selection of the commutation setting.

The torque versus current relationships for several commutation settings are shown in Fig. 11. It was found that by scaling the rms current, the curves matched each other rather well. Also, the change over from a square law in $i$ to an approximately linear relationship occurred at the same 50Nm torque level.

For a single phase carrying current $i$, with resistance $R$, and flux linkage $y$, the applied voltage is given by

$$V = iR + \frac{\partial y}{\partial t} \qquad (2)$$

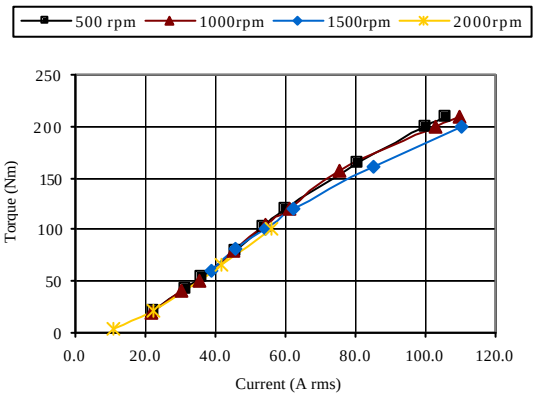


Fig. 7. Torque for commutation C2 ($\theta_{on}$ = 180°, $\theta_{off}$ = 30°)

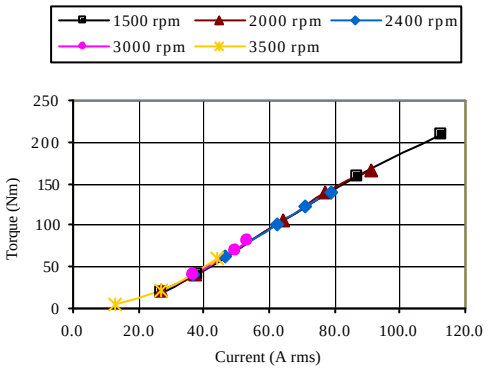


Fig. 8. Torque for commutation C3 ($\theta_{on}$ = 210°, $\theta_{off}$ = 60°)

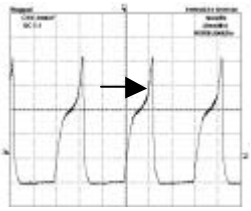

Fig. 9 Phase current (500 rpm, 200 Nm)
The arrow shows the on set of bulk saturation in the SRM

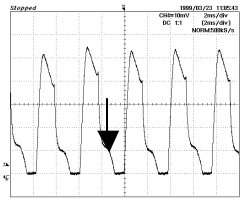

Fig. 10. Phase current (2000 rpm, 100 Nm)
The arrow shows a region that is causing a braking torque

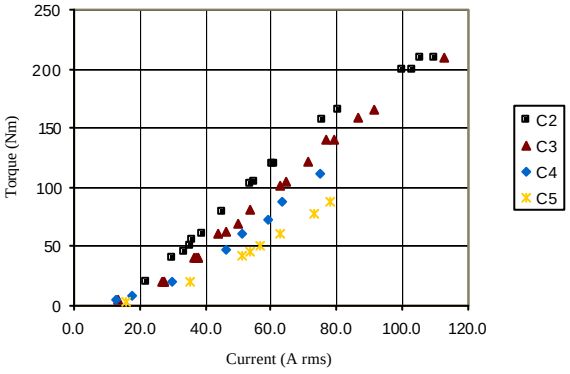


Fig. 11. Torque curves for commutation settings C2, C3, C4, C5

From knowledge of typical SRM voltage control waveforms and inspection of (2) it was reasoned that (3) may be a suitable approximation for the effective voltage.

$$V_{eff} = f_2(T)\mathrm{R} + f_1(T)w \qquad (3)$$

The effective voltage $V_{eff}$ is the average voltage applied to a phase during the on time ($\theta_{on}$ to $\theta_{off}$) and is the DC link voltage multiplied by the PWM duty cycle. Equation (3) is linear in speed $w$, where $f_2(T)R$ is the intercept and $f_1(T)$ is the gradient. So for a required torque $T$, the values of $f_2(T)$ and $f_1(T)$ are used to calculate the effective voltage and thus the required PWM duty cycle. Fig. 12 shows the measured effective voltage versus motor speed for commutation C2 and illustrates that (3) is a reasonable approximation. The last task is to define $f_2(T)$ and $f_1(T)$ for each of commutation setting. Function $f_2(T)$ is the average current during the on time and was determined from the torque versus current curves of Fig. 7 (for commutation C2). Function $f_2(T)$ was then used with (3) to calculate $f_1(T)$ for every measured data point and is shown in Fig. 13. Equations were fitted to the curves of Fig. 13 to give $f_1(T)$ for each commutation setting.

$$f_1(T) \quad = a_1 \sqrt{T} \qquad (T < 50) \qquad (4)$$
$$\quad = a_2 T^2 + a_3 T + a_4 \qquad (T \geq 50)$$

$$f_2(T) \quad = a_5 \sqrt{T} \qquad (T < 50) \qquad (5)$$
$$\quad = a_6 T + a_7 \qquad (T \geq 50)$$

We want to emphasise that (3) is only an approximation and that functions $f_2(T)$ and $f_1(T)$ are not dependent on torque alone. However, within the confines of our control structure and strategies, the correlation was strong enough for each of the motors in this particular application. In practice, (3) was extended to include the effects of temperature variation, circuit resistances and constant voltage drops. Also, there are other variations of (3), which give slightly better results.

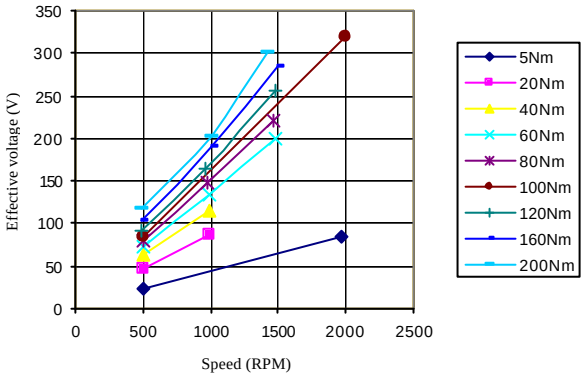


Fig. 12. Effective voltage for C2 ($\theta_{on}$ = 180°, $\theta_{off}$ = 30°)

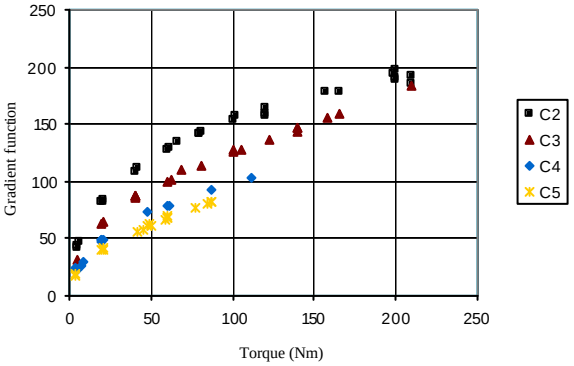


Fig. 13. Gradient function – $f_1(T)$

## CUSTOMISING EQUATIONS AND CAR TESTING

The fact that each SRM uses the same lamination, and only the number of turns, wire thickness, and motor length are changed, makes the task of customising the equations for each motor easier. If the number of turns in an SRM is doubled, then to maintain the same flux density (B) at a particular rotor position and operating point, the phase current is approximately doubled and the voltage is halved. If the SRM length is halved, then to maintain the same flux density at a particular rotor position and speed, the phase current is approximately the same, the torque is halved and the voltage is halved. Therefore, if we mathematically re-scale the torque versus current curves for each SRM (shown in Fig. 14) to fit the torque versus current curve of the prototype SRM, we can use the torque and current re-scaling factors to re-scale the prototype equations (3), (4), and (5) for each SRM.

Due to time constraints it was not possible to mount each SRM on a loading rig to verify its performance. The final SRMs were assembled in both cars, and a technique had to be developed to commission and test the individual systems. The ICE, disc brakes, and motoring and generating capabilities of the SRMs were all utilised to make the car its own loading rig for testing the individual systems. The rms current of the three phases were measured and averaged to give an estimate of the SRM torque at a particular steady state load point to confirm our set of motor equations. Most of the measured operating points fell within our targeted torque accuracy of 10%. In driving trials, the response and stability of the control system was as a driver would expect. Also, in most cases the transition from one commutation state to the next was undetectable to the driver.

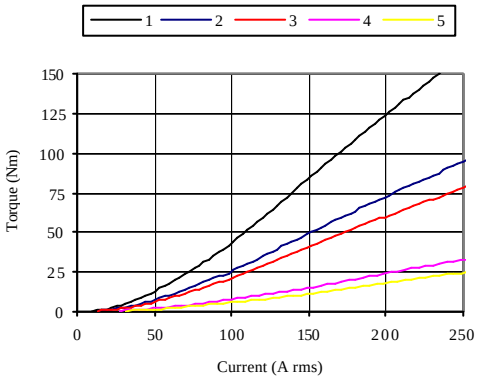


Fig. 14. FEA calculated torque versus current for C1
1 = aXcessaustralia LEV, main SRM
2 = aXcessaustralia LEV, capacitor SRM
3 = ECOmmodore, capacitor SRM
4 = aXcessaustralia LEV, battery SRM
5 = ECOmmodore, battery SRM

## CONCLUSION

This paper described the selection and development of a voltage-based control strategy for implementing average torque control of several SRMs in an HEV application. The SRMs and controllers performed as intended, were acoustically quiet, and gave the type of response and stability that a driver would expect. The aggressive time schedules and extensive publicity commitments of both cars dictated the use of a simple control strategy. The computational and memory requirements of this voltage-based control strategy are so low that it could be performed with a basic 8-bit microcontroller and a simple programmable logic device, or alternatively with a inexpensive DSP such as the Texas Instruments TMS320LF2402. If higher torque accuracy is desired and the dynamic requirements are modest, one solution may be to use the voltage controller described in this paper as a feed forward in combination with an rms current (or similar current quantity) control loop.

## ACKNOWLEDGMENTS

There are too many people involved in the project to name each person individually, but the authors would like to give collective thanks to:

- General Motors Holden Ltd.
- The aXcessaustralia LEV consortium of over 80 companies.
- The CSIRO research projects working on: Advanced Batteries, Super-Capacitors, Numerical Modelling, Atmospheric Modelling, Light Metal Castings, and Motor Design.

## REFERENCES

[1] http://www.holden.com.au/ecommodore
[2] D. Lamb, "The aXcessaustralia Hybrid Electric Car Project", *FISITA World Automotive Congress,* June 2000, Seoul, South Korea, Paper F2000H260
[3] K.M. Rahman, B. Fahimi, G. Suresh, A.V. Rajarathnam, M. Ehsani, "Advantages of Switched Reluctance Motor Applications to EV and HEV: Design and Control Issues," *IEEE trans Ind. App.*, Vol. 36.1, January 2000
[4] H.C. Lovatt and J.B. Dunlop, "Power Transfer in Hybrid Electric Vehicles with Multiple Energy Storage Units", *PEMD*, April 2002, Bath, UK
[5] H.C. Lovatt and J.M Stephenson, "Computer-optimized smooth-torque current waveforms for switched-reluctance motors", *IEE Proc. Electr. Power Appl.*, Vol. 144.5, September 1997
[6] P.G. Barrass and B.C. Mecrow, "Flux and torque control of switched reluctance machines" ", *IEE Proc. Electr. Power Appl.*, Vol. 145.6, November 1998
[7] W. Wu, H.C. Lovatt, and J.B. Dunlop., "Optimization of Switched Reluctance Motors for Hybrid Electric Vehicles", *PEMD,* April 2002, Bath, UK